

The Steady-State Characteristics of a Hydrostatic Thrust Bearing With a Floating Disk

M. Harada
Associate Professor.

J. Tsukazaki
Research Associate.

Department of Mechanical Engineering,
Faculty of Engineering,
Saitama University,
255 Shimo-Ookubo, Urawa, 338
Japan

To reduce the frictional power loss of hydrostatic thrust bearings, the hydrostatic thrust bearing with a floating disk shaped in a simplified configuration is proposed. And the load capacity and the frictional torque are experimentally investigated in laminar and superlaminar regimes. Following results can be obtained: (1) The disk floats at a certain stable position for given shaft rotational speed and rotates at nearly half rotational speed of the shaft. (2) The frictional torque of this type of the bearing is less than half of a conventional hydrostatic thrust bearing with the same surface configuration as the floating disk.

Introduction

This paper presents a proposal of the reduction of the frictional power loss for the hydrostatic thrust bearing operating in laminar and superlaminar regimes.

The hydrostatic thrust bearing with a floating disk as shown in Fig. 1 is proposed (we call this bearing "the floating disk bearing" in this paper). An idea similar to the floating disk can be seen in Fig. 2(a) and Fig. 2(b) [1, 2]. Figure 2(a) shows the hybrid fluid-film-rolling element bearing [1]. The bearing shown in Fig. 2(b) is the floating disk thrust bearing supported by the hydrodynamic film forces [2]. But the floating disk supported by hydrodynamic forces often comes into contact with either the bearing or the rotor surface [2].

A floating disk supported by hydrostatic forces can rotate at a stable oil film thickness for any given rotational speed. But, in the range of high shaft rotational speed, the effect of the centrifugal force upon the oil film makes the remarkable change in the load capacity and the stiffness [3, 4, 5]. Moreover, as the configuration of the floating disk is very complicated with the recesses, the drain holes and the restrictors, the disk is difficult to be made.

In this paper, the simplified floating disk is proposed and the load capacity, the disk rotational speed and the frictional torque of the hydrostatic thrust bearing with a floating disk are experimentally investigated. Moreover, the characteristics of the conventional hydrostatic thrust bearing with the same surface configuration as the floating disk are measured by fixing the disk at the bearing plate (we call this bearing "the conventional bearing" in this paper).

Experimental Apparatus

The experimental apparatus are shown in Fig. 3. The rotor

① is mounted on a vertical driving shaft supported by angular-type ball bearings. The bearing plate ② and the floating disk ③ have 100 mm outer diameter and 32 mm inner diameter. The floating disk has 6 sectorial recesses with 92 mm outer diameter, 56 mm inner diameter, 44 degrees angular span and 0.5 mm in depth as shown in Fig. 4. The lubricant supplied to the upper groove of the disk also flows into the lower one through the 2 mm diameter holes. The lubricant is supplied to the both disk surfaces through the inner lands and the restrictors. The restrictor is shaped into the channel. It is 0.5 mm wide, 0.3 mm deep and 8 mm long. Instead of the

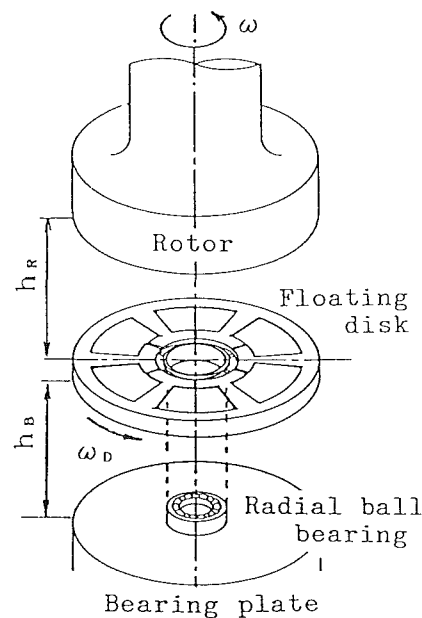


Fig. 1 Hydrostatic thrust bearing with a floating disk

Contributed by the Tribology Division of THE AMERICAN SOCIETY OF MECHANICAL ENGINEERS and presented at the ASME/ASLE Joint Tribology Conference, Baltimore, Md., October 16-19, 1988. Manuscript received by the Tribology Division April 10, 1988. Paper No. 88-Trib-30.

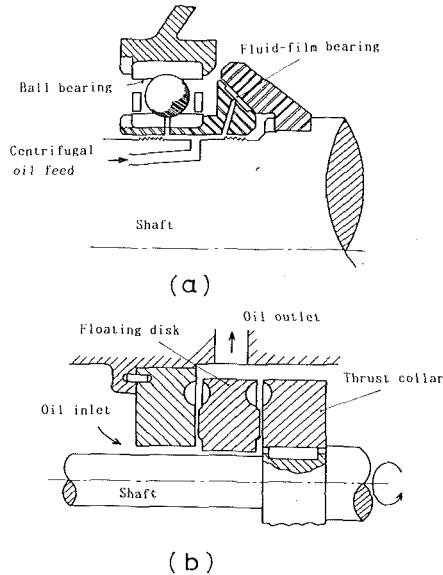


Fig. 2 Another proposals for reducing frictional torque

channel restrictor, we can put a capillary tube in the same position as the channel.

The floating disk has a radial ball bearing and is attached to the bearing plate through the ball bearing. The inner race of the ball bearing can be moved smoothly in the axial direction.

The displacement of the bearing plate and the floating disk are measured by three eddy-current-type displacement detectors (4) arranged at angular intervals of 120 degrees. The bearing plate is supported by the stroke bearing (5) which can be rotated in the radial direction and moved in the axial direction. The stroke bearing is mounted on three poles with 0.5 mm pitch adjusting screws (6). The radial/axial displacement of the rotor is smaller than 2.0 μm within the test speed range of 0 to 14,000 r/min. The bearing plate is adjusted parallel within an error of 2.0 μm to the surface of the rotor by turning the above-mentioned 0.5 mm pitch adjusting screws for every rotational speed and load. A load of 0 to 1.2 kN can be applied to the test bearing.

The low kinematic viscosity lubricant ($\nu = 2.6 \times 10^{-6} \text{m}^2/\text{s}$, at 35°C) is used. The feed pressure is 200 kPa. Inlet and outlet temperatures are measured by copper-constantan ther-

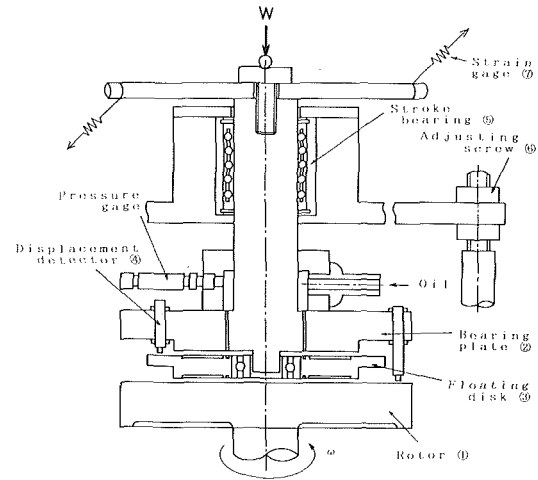


Fig. 3 Experimental apparatus

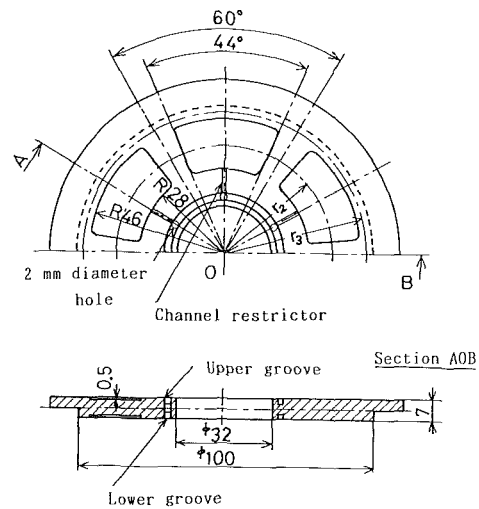


Fig. 4 Detail drawing of the floating disk

mocouples. Inlet temperature is kept constant at $35 \pm 2^\circ\text{C}$. The maximum outlet temperature of the conventional bearing is 43°C . Then, the inlet temperature is taken as the temperature of the lubricant in the recess and on the land.

Nomenclature

h^* = bearing clearances at the land or at the recess	y = coordinate perpendicular to the bearing surface	W = bearing load, N
K = coefficient of discharge of the restrictor	h = bearing clearance of the conventional bearing or the floating disk bearing = $h_B + h_R$	θ = angular coordinate
l = length of the restrictor m	h_B = clearance between the disk and the bearing plate	μ = viscosity of lubricant Pa·s
p = pressure Pa	h_R = clearance between the disk and the rotor	ρ = density of lubricant kg/m ³
p_0 = outlet pressure of the restrictor Pa	H_0 = depth of the recess	τ = shear stress N/m ²
p_s = supply pressure Pa	H = $H_0 + h$	ϵ_n = ratio of the disk rotational speed to the shaft speed = ω_D/ω
R = outer diameter of the floating disk m	H_B = $H_0 + h_B$	ω = shaft rotational speed, rad/s
r = radial coordinates m	r_2 = average radius of the recess, m	ω_c = critical rotational speed, rad/s
r_i = inner diameter of the recess m	r_3 = average radius of the land, m	ω_D = disk rotational speed, rad/s
r_0 = outer diameter of upper/lower groove m	Re_2 = Reynolds number in the recess = $\omega r_2 H_B/\nu$ or $\omega r_2 H/\nu$	ν = kinematic viscosity, m ² /s
u = velocity component in the circumferential direction m/s	Re_3 = Reynolds number on the land = $\omega r_3 h_B/\nu$ or $\omega r_3 h/\nu$	
w = velocity component in the radial direction m/s	T = frictional torque, N·m	
		Subscripts
		B = values at bearing plate side or at bearing plate
		R = values at rotor side or at rotor surface
		D = values at floating disk surface
		m = mean

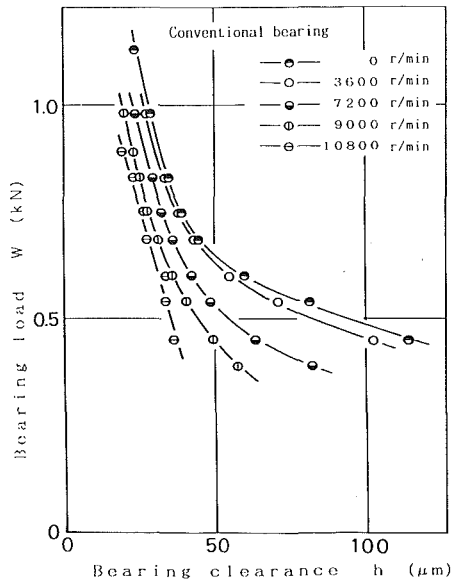


Fig. 5 Bearing load of the conventional bearing versus bearing clearance h

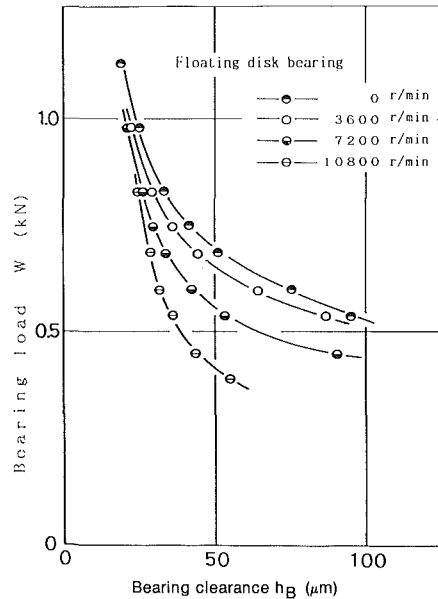


Fig. 7 Bearing load of the floating disk bearing versus bearing clearance h_B

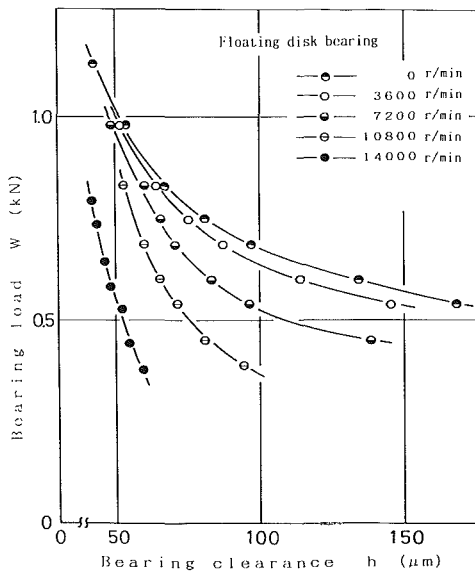


Fig. 6 Bearing load of the floating disk bearing versus bearing clearance h

The frictional torque of the test bearing is measured by strain gages (7). On the upper surface of the disk, there are two aluminum foil about $20 \mu\text{m}$ thick and 5 mm wide. When a foil runs below the displacement detector, it detects the thickness of the foil and generates a pulse. The rotational speed of the floating disk can be known by counting the number of the pulse per second.

Experimental Results

Load Capacity. In order to investigate if this type of hydrostatic thrust bearing will function properly as a bearing, the load capacities are examined. Figure 5 shows the load capacity of the conventional bearing. When the shaft does not rotate, the load capacity does not tend to zero, but to a certain constant value for the large clearance. When the shaft rotates, the load capacities are reduced with increase of the shaft rotational speed. Anyway, we can consider that the conventional thrust bearing will function as a bearing.

Figures 6 and 7 depict the load capacities of the hydrostatic

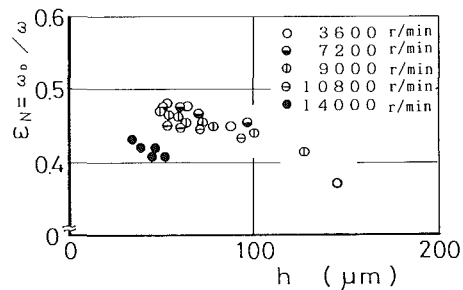


Fig. 8 Ratio of the disk rotational speed to the shaft rotational speed

thrust bearing with a floating disk as a function of h and h_B , as well as shaft rotational speed. The influence of the shaft rotational speed upon the load capacity is almost the same as the one upon the load capacity of the conventional bearing. Then, we consider that the hydrostatic thrust bearing with a floating disk also functions as a bearing. Comparing Fig. 7 with Fig. 6, we can consider that the disk floats at a certain stable position between $h_B/h = 0.4$ and 0.6 for the given shaft rotational speed.

Figure 8 shows the ratio of the disk rotational speed to the shaft speed for the clearance h . As the clearance increases, the disk rotational speed has a tendency to decrease. And in the range of this experiment, the disk has a stable rotational speed about 45 to 60 percent of the shaft speed.

Frictional Torque. Figure 9 shows the experimental results of the frictional torque as a function of the bearing load, as well as shaft rotational speed. In this figure, the frictional torques of the hydrostatic thrust bearing with a floating disk are compared with the one of the conventional bearing. The four types of Reynolds numbers are also added in this figure. $Rec = \omega_c r h / \nu = 1,500$ is taken as a critical Reynolds number of the lubricant film [6]. As the shaft rotational speed increases, the transition occurs in the recess first and then, at higher rotational speeds, the flow on the land becomes superlaminar. In the superlaminar or turbulent regime, the frictional torque does not only increase with increase of the shaft rotational speed, but also increases with increase of the Reynolds number.

When the flow in the recess of the conventional bearing

becomes superlaminar, its frictional torque becomes larger than that in the laminar regime. This tendency becomes more pronounced as the Reynolds number increases (see Fig. 9(a), (b), and (c)). In the higher Reynolds number region, the transition occurs in the flow on the land of the conventional bearing. As a result, the frictional torque increases significantly. In the light load region, or the large clearance one, the Reynolds number at high shaft rotational speed is large. The frictional torque, then, becomes very large in this region as shown in Fig. 9(d) and (e).

In case of the hydrostatic thrust bearing with a floating disk, the frictional torque is half even in the laminar regime. This is because the relative velocity is one-half. Moreover, as Reynolds number is one-half of the conventional bearing, the critical shaft rotational speed is two times that of the conventional bearing. Even if the transition occurs in the recess, the frictional torque of the bearing in the low Reynolds number region remains nearly the same as that in the laminar regime. Thus, the frictional torque of the floating disk bearing is nearly half of the conventional bearing as shown in Fig. 9(a). At higher Reynolds numbers, the influence of the Reynolds number upon the frictional torque of the bearing becomes more noticeable. As a result, the frictional torque of the floating disk bearing becomes less than a half that of the conventional bearing as shown in Fig. 9(b) and (c).

Even under the condition that transition from laminar to superlaminar flow occurs on the land of the conventional

bearing, the lubricant flow on the land of the floating disk bearing remains in the laminar regime over the rotational speed range. In this region, the ratio of the frictional torque of the floating disk bearing to that of the conventional bearing becomes one-third or less as shown in Fig. 9(d) and (e).

Conclusions

To reduce the frictional power loss of the hydrostatic thrust bearing, the hydrostatic bearing with a floating disk is proposed. The limited experimental data presented here show that the disk floats at $h_B/h = 0.4$ to 0.6 and rotates at about one-half the shaft rotational speed. The floating disk bearing has about one-half the frictional torque of the conventional bearing. The floating disk is especially effective in the superlaminar and turbulent regimes.

References

- 1 Nypan, L. J., Hamrock, B. J., Scibbe, H. W., and Anderson, W. J., "Optimization of Conical Hydrostatic Bearing for Minimum Friction," ASME JOURNAL OF LUBRICATION TECHNOLOGY, Vol. 94, Apr. 1972, pp. 136-142.
- 2 Official report for the patent No. 222616, 1984, 57-63 (in Japanese).
- 3 Dowson, D., "Inertia Effects in Hydrostatic Thrust Bearings," ASME Journal of Basic Engineering, Vol. 83, June 1961, pp. 227-234.
- 4 Harada, M., Aoki, H., Hongo, T., and Suda, M., "Turbulent Shear Flow in Hydrostatic Thrust Bearings," Bull. JSME, Vol. 24, No. 118, 1981, pp. 420-426.
- 5 Harada, M., Miyaji, R., and Anada, Y., "Turbulent Lubrication for a

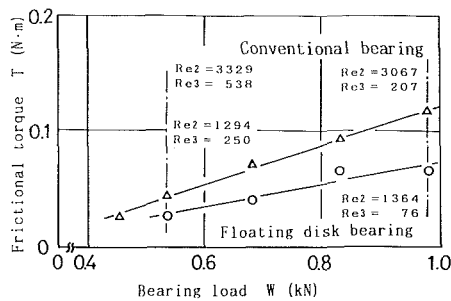


Fig. 9(a) 3600 r/min

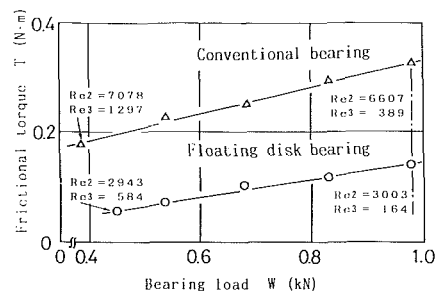


Fig. 9(b) 7200 r/min

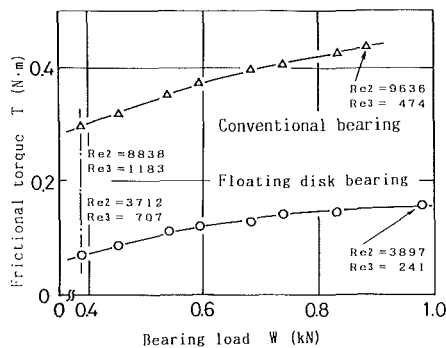


Fig. 9(c) 9000 r/min

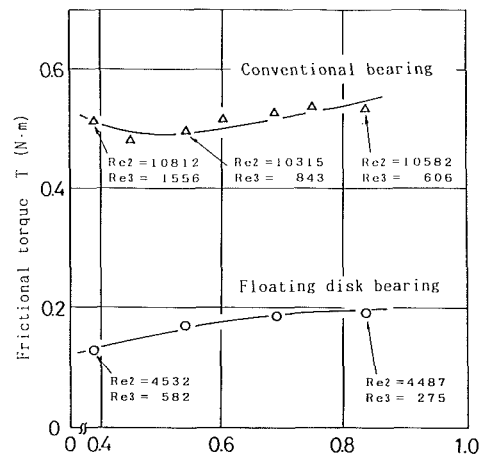


Fig. 9(d) 10800 r/min

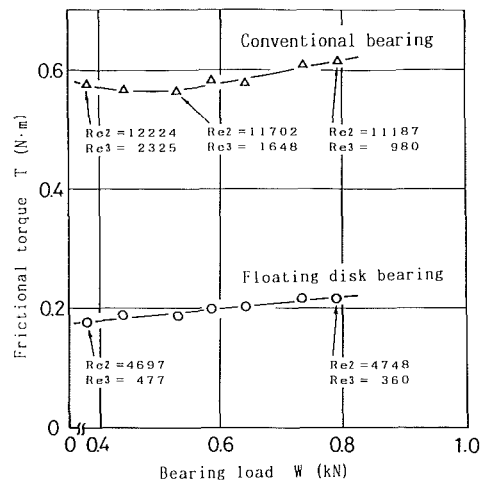


Fig. 9(e) 14000 r/min

Fig. 9 Frictional torque of the floating disk bearing and the conventional bearing versus bearing load

Hydrostatic Thrust Bearing with a Circular Recess," *JSM E International Journal*, Vol. 30, No. 269, 1987, pp. 1819-1825.

6 Harada, M., Aoki, H., and Suda, M., "Inertia Effects in the Turbulent Shear Flow of the Lubricant Film," *Bull. JSME*, Vol. 23, No. 175, 1980, pp. 90-96.

7 Harada, M., Tsukazaki, J., Suda, M., and Kimura, M., "Thrust Bearing with a Hydrostatic floating Disk," *Trans. JSME* (in Japanese), submitted.

APPENDIX

In laminar regime, replacing the channel restrictor with a capillary tube with the same hydraulic radius, characteristics of the floating disk bearing and the conventional bearing can be approximately calculated [7].

The equations of motion including a centrifugal inertia term are

$$0 = -\frac{1}{r} \cdot \frac{\partial P}{\partial \theta} + \mu \frac{\partial^2 u}{\partial y^2} \quad (1)$$

$$-\frac{\rho u^2}{r} = -\frac{\partial P}{\partial r} + \mu \frac{\partial^2 w}{\partial y^2} \quad (2)$$

Assuming that the influence of the pressure gradient in the circumferential direction upon the velocity in the radial direction is negligible and integrating equations (1) and (2) with the boundary conditions

$$u = r\omega_0 \text{ at } y = 0, \quad u = r\omega \text{ at } y = h^*,$$

$$w = 0 \text{ at } y = 0 \text{ and } w = 0 \text{ at } y = h^*$$

the non-dimensional-mean velocities can be obtained as follows:

$$\bar{u}_m = \frac{u_m}{h^* r \omega} = -\frac{h^{*2}}{12\mu r \omega} \cdot \frac{\partial P}{\partial (r\theta)} + \frac{1}{2} \left(1 + \frac{\omega_0}{\omega}\right) \quad (3)$$

$$\bar{w}_m = \frac{w_m}{h^* r \omega} = -\frac{h^{*2}}{12\mu r \omega} \cdot \frac{\partial P}{\partial r} + \frac{1}{40} \frac{\omega h^{*2}}{\nu} \left\{ \left(1 - \frac{\omega_0}{\omega}\right)^2 + \frac{10}{3} \cdot \frac{\omega_0}{\omega} \right\} \quad (4)$$

The shear stress in the circumferential direction is

$$\tau = \pm \frac{h^*}{2r} \cdot \frac{\partial P}{\partial \theta} \cdot (h^* - 2y) + \mu \frac{r\omega}{h^*} \cdot \left(1 - \frac{\omega_0}{\omega}\right) \quad (5)$$

The frictional torque becomes

$$T = \iint \left[\pm \frac{h^*}{2r} \cdot \frac{\partial P}{\partial \theta} + \mu \frac{r\omega}{h^*} \cdot \left(1 - \frac{\omega_0}{\omega}\right) \right] r^2 d\theta dr \quad (6)$$

Then, the nondimensional torque can be obtained as follows:

$$\bar{T} = \frac{T \cdot h}{\mu \omega R^4} = \iint \left[\pm \frac{h h^*}{2\mu \omega R^2 \cdot r'} \cdot \frac{\partial P}{\partial \theta} + \frac{h}{h^*} \cdot r' \cdot \left(1 - \frac{\omega_0}{\omega}\right) \right] r'^2 d\theta dr' \quad (7)$$

where

$$r' = \frac{r}{R}$$

Including the centrifugal effect, the flow rate through the capillary tube is

$$Q = K \left\{ P_s - P_0 + \frac{\rho \omega^2 \ell}{2} (r_i + r_0) \right\} \quad (8)$$

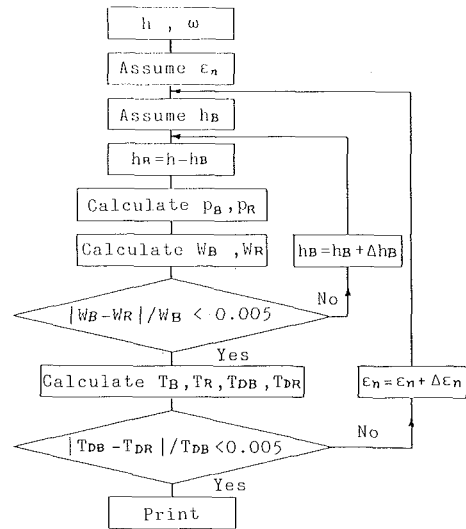


Fig. 10 Flow chart of computation

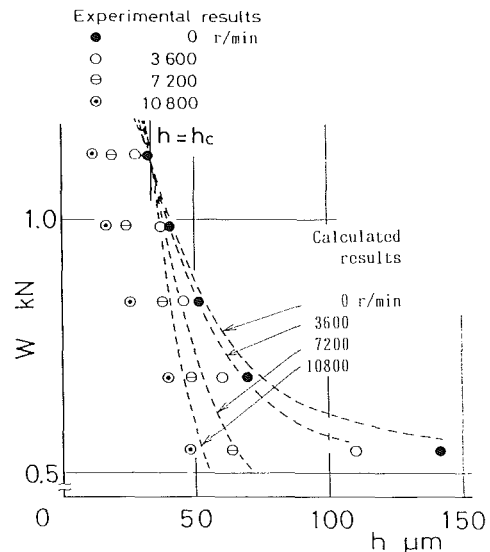


Fig. 11 Bearing load of the conventional bearing versus bearing clearance h

Applying equations (3), (4), (7), and (8) to the floating disk bearing and adopting the divergent formulation method, we can obtain the characteristics of the floating disk bearing. The flow chart of computation is shown in Fig. 10.

The calculated results and experimental data in the laminar regime are shown in Figs. 11 to 14. The experiments in the laminar regime are performed by applying the high kinematic viscosity lubricant ($\nu = 1.0 \times 10^{-5} \text{ m}^2/\text{s}$ at 35°C) to the same floating disk bearing as that in the present paper. In this case, the rotation of the shaft raises the outlet temperature of the lubricant for constant inlet temperature (35°C) and makes the lubricant viscosity decrease (Table 1). The previous results [5] show the lubricant temperature for the greater part of flow field of the bearing clearance approximately equal to the outlet temperature. Then, corrections for the lubricant viscosity are made by using the average outlet temperatures for each rotational speed.

Figures 11 to 13 show the load capacity. In the hydrostatic thrust bearing with a concentric circular recess, the influences of the shaft rotational speed upon the bearing characteristics are summarized as follows [5]:

- (1) The centrifugal force acting on the lubricant flow in

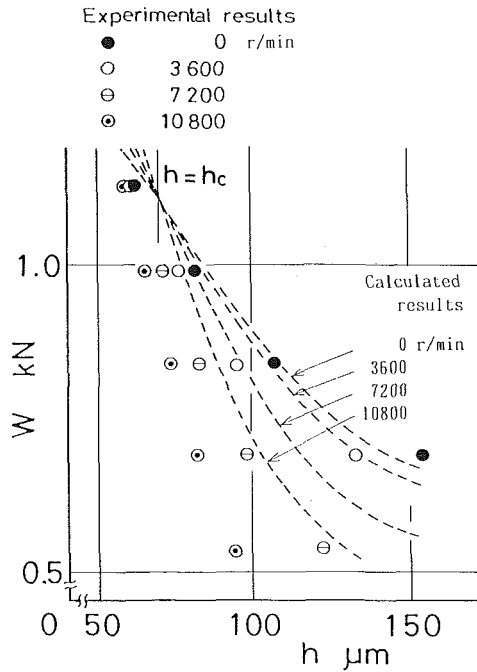


Fig. 12 Bearing load of the floating disk bearing versus bearing clearance h

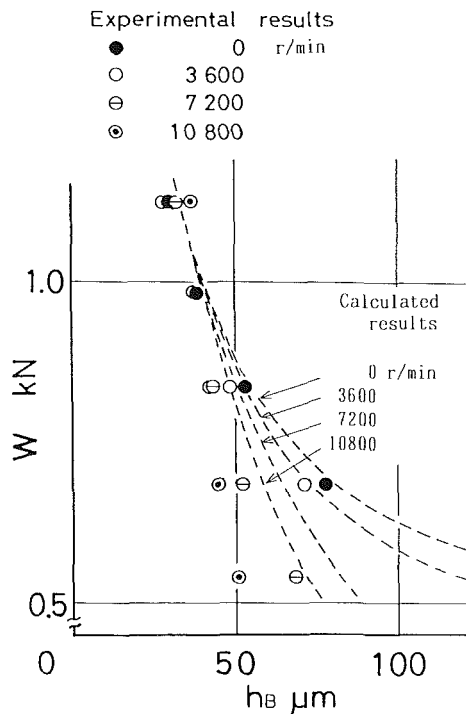


Fig. 13 Bearing load of the floating disk bearing versus bearing plate side clearance h_B

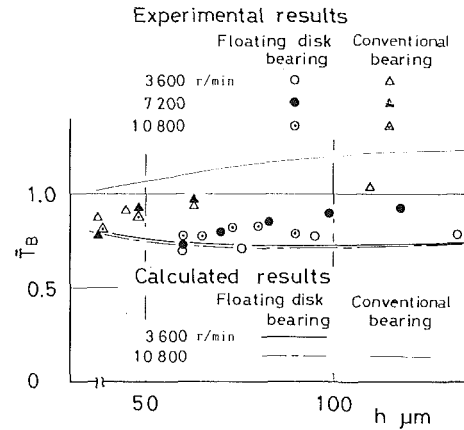


Fig. 14 Nondimensional torque versus bearing clearance h

Table 1 Kinematic viscosity

Shaft speed, r/min	$\nu \times 10^5 \text{ m}^2/\text{s}$		
	3600	7200	10800
Conventional bearing	0.97	0.73	0.63
Floating disk bearing	1.0	0.84	0.73

the recess makes the pressure increase with an increase of the radius.

(2) It also makes the lubricant flow rate increase and the pressure at the outlet of the restrictor decrease. As a result, the load capacity decreases with an increase of the rotational speed. This tendency is remarkable in the large lubricant film thickness region.

On the other hand,

(3) The positive pressure gradient in the radial direction generated in the recess causes the load capacity to increase.

The effects (1) and (2) are changed with (3) at a certain lubricant film thickness h_c . In the range of $h > h_c$, the load capacity decreases with increase of the rotational speed. But, in the range of $h < h_c$, the rotation of the shaft makes the load capacity increase.

The same tendencies are shown in case of the calculated results of the conventional bearing and the floating disk bearing. But, as the shaft rotational speed and the lubricant film thickness influence upon the coefficient of discharge of the channel restrictor, the experimental results do not quantitatively agree with the calculated ones. Thus, it is considered that the conventional bearing and the floating disk bearing will function as thrust bearings.

Figure 14 shows the nondimensional torque. There are little difference between the nondimensional torque of the conventional bearing and that of the floating disk bearing. But, as the clearance h of the floating disk bearing is approximately two times that of the conventional bearing and non-dimensional torque is expressed as $T_B \cdot h / \mu \omega R^4$, it can be considered that the enlargement of the clearance caused by the floating disk makes the frictional torque T_B decrease.